Computational fluid dynamics methodology for characterisation of leading edge erosion in whirling arm test rigs

IOP Conf. Series: Journal of Physics: Conf. Series **1222** (2019) 012011 doi:10.1088/1742-6596/1222/1/012011

Computational fluid dynamics methodology for characterisation of leading edge erosion in whirling arm test rigs

R Herring[1], K Dyer[1], A MacLeod[1] and C Ward[2]

[1] Offshore Renewable Energy Catapult, Offshore House, Albert Street, Blyth, NE24 1LZ, UK
[2] Department of Aerospace Engineering, Queen's Building, University of Bristol, Bristol, BS8 1TR, UK

robbie.herring@ore.catapult.org.uk

Abstract. Blade leading edge erosion has developed into a significant issue for the offshore wind industry. Protection solutions, including polymer coatings and tapes, are often applied to increase the blade lifetime. Experimental evaluation of protection systems is typically conducted in whirling arm rain erosion test rigs. Currently, there is no thoroughly validated method to relate the test results to real-world erosion performance. Furthermore, the design of rigs is not sufficiently limited to enable comparison of results between different rigs. Industry guideline, DNV-GL-RP-0171, provides a comparison method to address this issue. This paper describes the development of a droplet particle tracking Computational Fluid Dynamics methodology for rain erosion test rigs, which models the impact strike characteristics of a droplet, the number of impacts and the effect of rig aerodynamics. The methodology was applied to two rigs with different aerodynamics. Rain erosion tests were conducted in the rigs on identical coating and aluminium samples. The results were compared against predicted number of impacts from the DNV-GL guideline. Contradictory results were found, concluding that the guideline does not provide an accurate comparison between all test rigs, as it does not account for rigs where large aerodynamic effects cause droplet concentrations or droplet break-up.

1. Introduction

Blade leading edge erosion has developed into a significant issue for the offshore wind industry. Raindrops, hailstones or other particles impacting the blade leading edge cause material to be removed from the blade surface, leaving a rough profile that degrades the aerodynamic performance and impacts the structural integrity of the blade [1].

There are several erosion protection systems available to the industry that can increase the lifetime of the turbine by mitigating leading edge erosion, including coatings, tapes and soft shells. Experimental evaluation of protection systems is typically conducted in a whirling arm rain erosion test rig where a sample is fixed to the end of an arm and rotated through a rain field of a uniform droplet size [2].

Current test procedures and facilities remain limited to comparison of product performance under selected test conditions. Currently, there is no thoroughly validated method to relate test results to real-world erosion performance. Furthermore, industry standards, ASTM-G73, ISO-TS-19292-2, do not

limit the design of the rigs and the choice of test parameters to allow direct comparison of test results between different test rigs. Although industry guideline, DNV-GL-RP-0171 [3], does give a comparison method it does not account for rigs where large aerodynamic effects and droplet concentrations occur. This has been observed to lead to conflicting rain erosion test results due to the elastic and viscoelastic nature of polymer coatings.

For the development of a realistic lifetime prediction model from rain erosion test results, which accounts for all protection systems and rain erosion rigs, a direct relationship needs to be established between test rig parameters and the characteristics of the erosion developed in different materials. Testing then needs to be completed in a realistic accelerated rain erosion test correlated directly to the measured offshore wind turbine droplet impact environment.

In this work, a droplet particle tracking Computational Fluid Dynamics (CFD) methodology has been developed for rain erosion tests rigs. The methodology enables modelling of the impact characteristics of a droplet, the number of impacts and the effect of test rig aerodynamics. Two whirling arm test rigs have been evaluated:

- A previous configuration of the test rig at the Energy Technology Centre (ETC).
- The test rig at Offshore Renewable Energy (ORE) Catapult. This rig is the wind industry standard design used within the DNV-GL guideline for geometrical droplet impact calculations.

2. ETC Test Rig Model

2.1. Model Description

A 3D model of the previous configuration of the whirling arm test rig at the ETC was constructed in ANSYS Fluent CFD. The ETC rig possessed two arms with either flat or aerofoil samples. This was updated to a single arm running the same aerofoil samples as the ORE Catapult rig for testing. The test room was simplified to a circular space and the motor support was approximated to an equivalent circular cone. These approximations enable the rotating rig to be modelled using a rotating reference frame within the CFD model. Since the rig is rotationally symmetrical, a periodic boundary was used along the arm centreline, halving the computational mesh size. The flow solutions have been solved in steady-state. Figure 1 presents the CFD model of the test rig with contours of velocity magnitude highlighted. The circumferential line illustrates the droplet release positions.

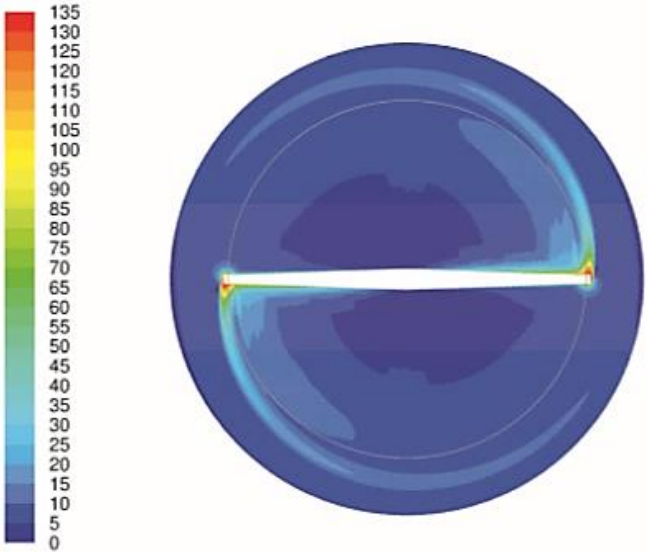

Figure 1. CFD model of ETC test rig, with contours of velocity magnitude on a horizontal plane level with the sample centreline (m/s) highlighted.

The local flow velocities acting on the droplet and the resulting motion of the droplet were predicted using a Matlab model. Droplets are released, and their equations of motion solved in the time domain as they pass through the varying velocity field. At each time step, the aerodynamic force on the droplet is calculated via a drag law. This drag force is added to the gravitational force and used to calculate the droplet acceleration, which is then integrated through time to calculate the trajectory. There is a risk that the aerodynamic forces experienced by the droplets as they travel through the rig may result in their breakup. To account for this, a droplet breakup criterion was implemented based on the Weber number [4]. Combining the droplet tracking with the CFD model predicts the aerodynamics effects of the test rig on falling droplets and its resulting impact characteristics.

2.2. ETC Test Rig Aerodynamics

Two test sample configurations have been repeated in the CFD model: a vertical flat plate and an aerofoil sample, both tested at 700 rpm. These cases were selected to provide a good understanding of the dominant features of the droplet behaviour and the degree to which this can be captured accurately in the modelling.

Figure 2 shows the track of streamlines over the two samples at 700 rpm. The streamlines around the flat plate sample highlight the influence of the clamping block on the flow into the centre of the sample. Furthermore, the streamlines passing over the sample indicate that the combination of the clamp and sample wake is causing rotation in the wake behind the sample. This is evident by the loop of streamlines above the sample. The aerofoil also introduces rotation into its wake due to its tip vortex. These rotational effects, along with the severe shear between the sample wake and the surroundings, influence the droplet tracks and their likelihood of breaking up along their trajectory towards the sample.

Droplets were released from needles around the full 360° of the rig at the radial location corresponding to the specimen centre. Each droplet track stops when it either strikes the sample or leaves the annular region around it. The droplet impacts on the sample were recorded and have been visualised in Figure 3.

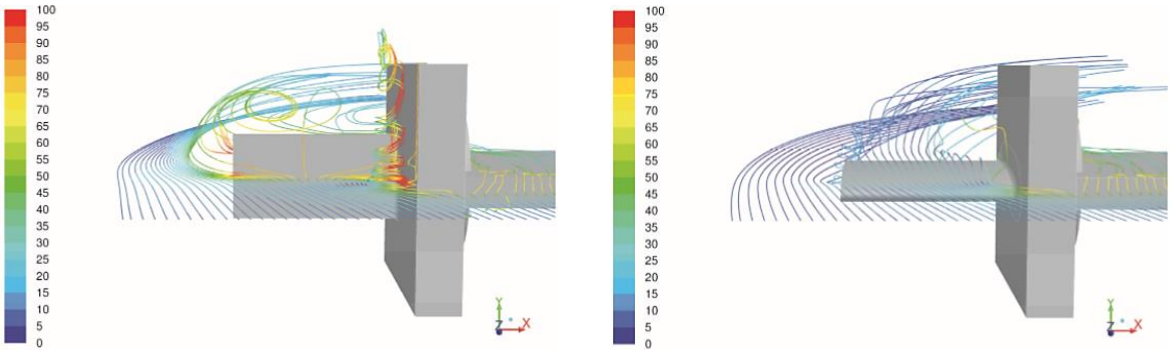

Figure 2. Flow streamlines coloured by velocity magnitude (m/s) for the flat plate (left) and the aerofoil sample (right).

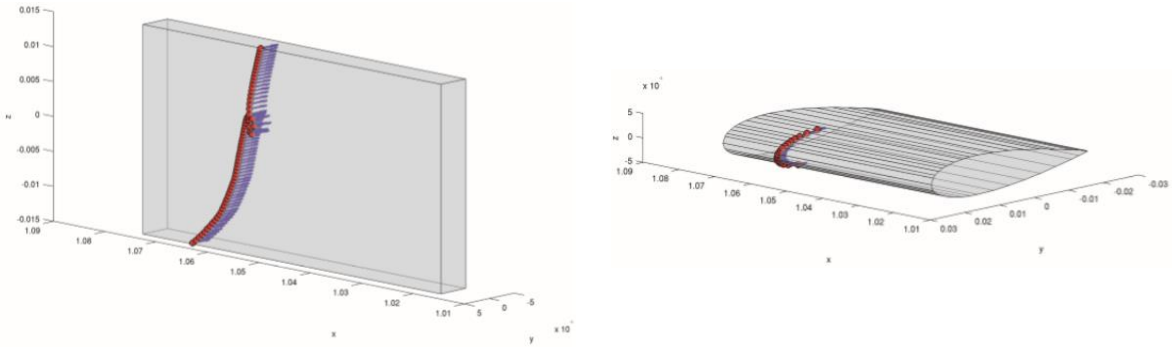

Figure 3. Droplet impact locations on the flat plate (left) and the aerofoil sample (right) determined computationally.

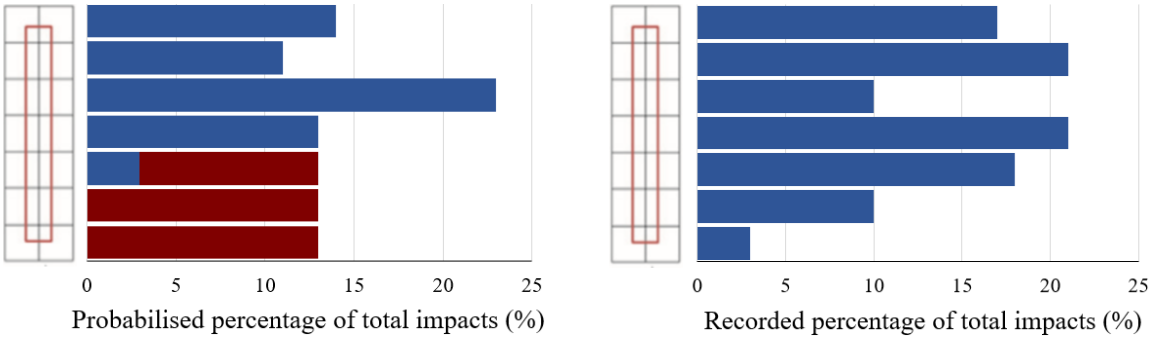

Figure 4. Histograms presenting the impact locations determined computationally (left) and experimentally (right) on the flat plate.

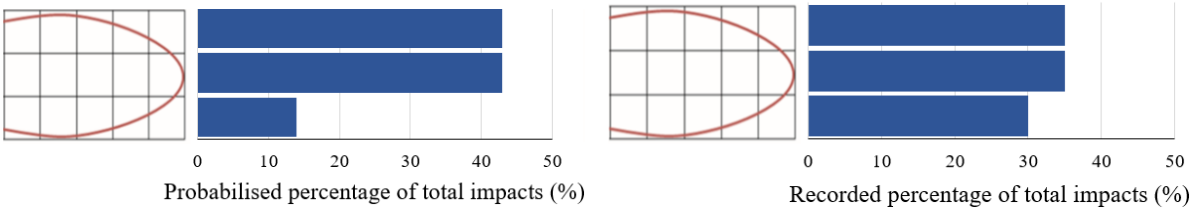

Figure 5. Histograms presenting the impact locations determined computationally (left) and experimentally (right) on the aerofoil sample.

In the flat plate results, a loop can be seen in the impact locations, introducing droplet concentrations onto the sample. The model shows that the droplets whose impacts form this loop are affected by the passage of the previous sample as they are released from the needles. This effect, combined with the uneven aerodynamic flow across the sample, cause the droplet to veer from its straight trajectory. In the aerofoil sample, the droplet impact path has moved outwards radially from the central droplet release position.

2.3. Model Validation

Validation was performed by comparing the number of droplet impacts and strike locations on a sample in the ETC test rig and the developed CFD model. High speed video cameras were used in the test rig to examine the droplet impacts and locations, both radially and longitudinally along the sample.

The vertical positions of the impact points have been collated into histograms which were compared with the results from the ETC rig (Figure 4 and Figure 5). Droplet breakup has been presented in red. The CFD model gave consistent results with the high-speed video measurements.

3. ORE Catapult Test Rig Model

3.1. Model Description

Using the validated methodology, a CFD model for the ORE Catapult test rig was developed. This rig possesses three arms with an aerofoil sample positioned along each arm. Figure 6 presents the CFD model of the test rig with contours of velocity magnitude highlighted. The circumferential lines illustrate the ten droplet release positions. The sample has a length of 0.45 m and is situated 0.8 m along each rotating arm.

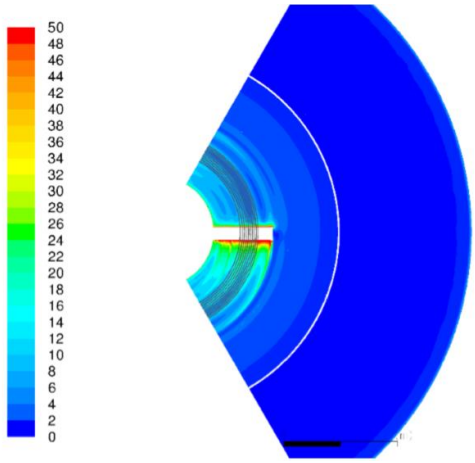

Figure 6. CFD model of ORE Catapult test rig, with contours of velocity magnitude on a horizontal plane level with the sample centreline (m/s) highlighted.

3.2. ORE Catapult Test Rig Aerodynamics

Contours of radial velocity can be seen across the plane of the sample. This demonstrates that the rotating blade causes an outward flow across the wake. Slight steps at each end of the sample result in small regions of separated flow at both ends of the sample. Figure 7 reveals that the flow over the sample and arm is streamlined and produces only a thin wake. This aerodynamic performance is significantly better than the flow results from the previous configuration of the ETC test rig. This can be attributed to the clean mounting design and aerofoil shaped sample.

The even aerodynamic flow over the sample and the thin wake is unlikely to affect the droplet trajectories. However, the outward flow and small regions of flow separation may influence the motion of the droplets. Their influence has been investigated.

Figure 8 presents the impact location of droplets along a test sample at 1000 rpm. The droplets can be seen to impact the sample at regular intervals with minimal scatter. To understand the magnitude of the scatter at different rotational velocities, the positions of the impact points have been collated into histograms (Figure 9). At all rotational velocities, the ten points of droplet release can be seen clearly. The histograms reveal that the aerodynamic forces present in the rig do cause some slight scatter. This effect becomes more pronounced at higher velocities due to a greater outward flow across the wake. However, the clear impact points demonstrate that the aerodynamic forces are minimal and do not govern the droplet flow. As a result, it can be determined that the ORE Catapult test rig does not experience aerodynamic droplet concentrations.

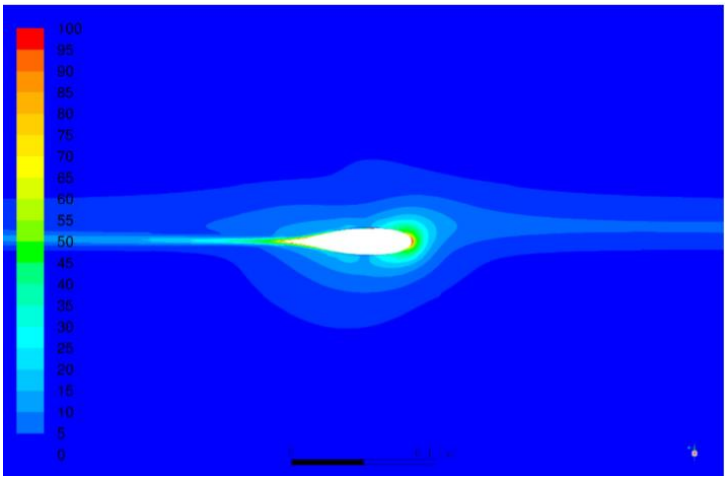

Figure 7. Contours of velocity magnitude (m/s) on the aerofoil sample used in the ORE Catapult test rig.

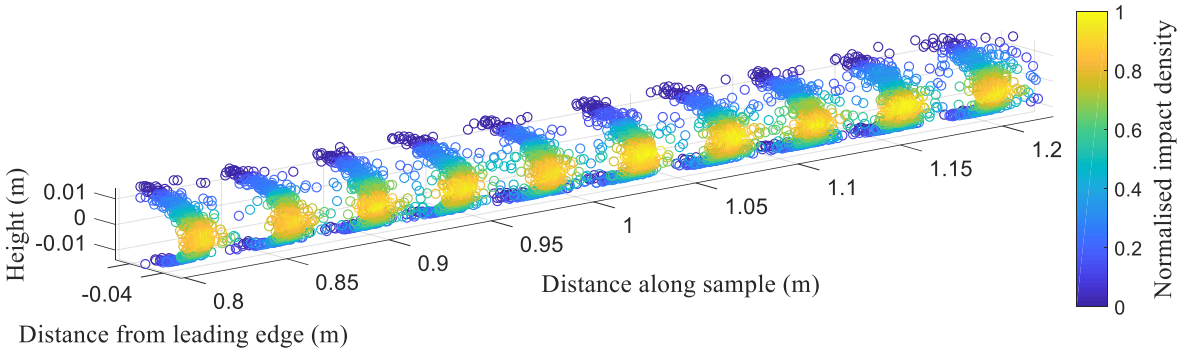

Figure 8. Droplet impact location on a sample in the ORE Catapult test rig.

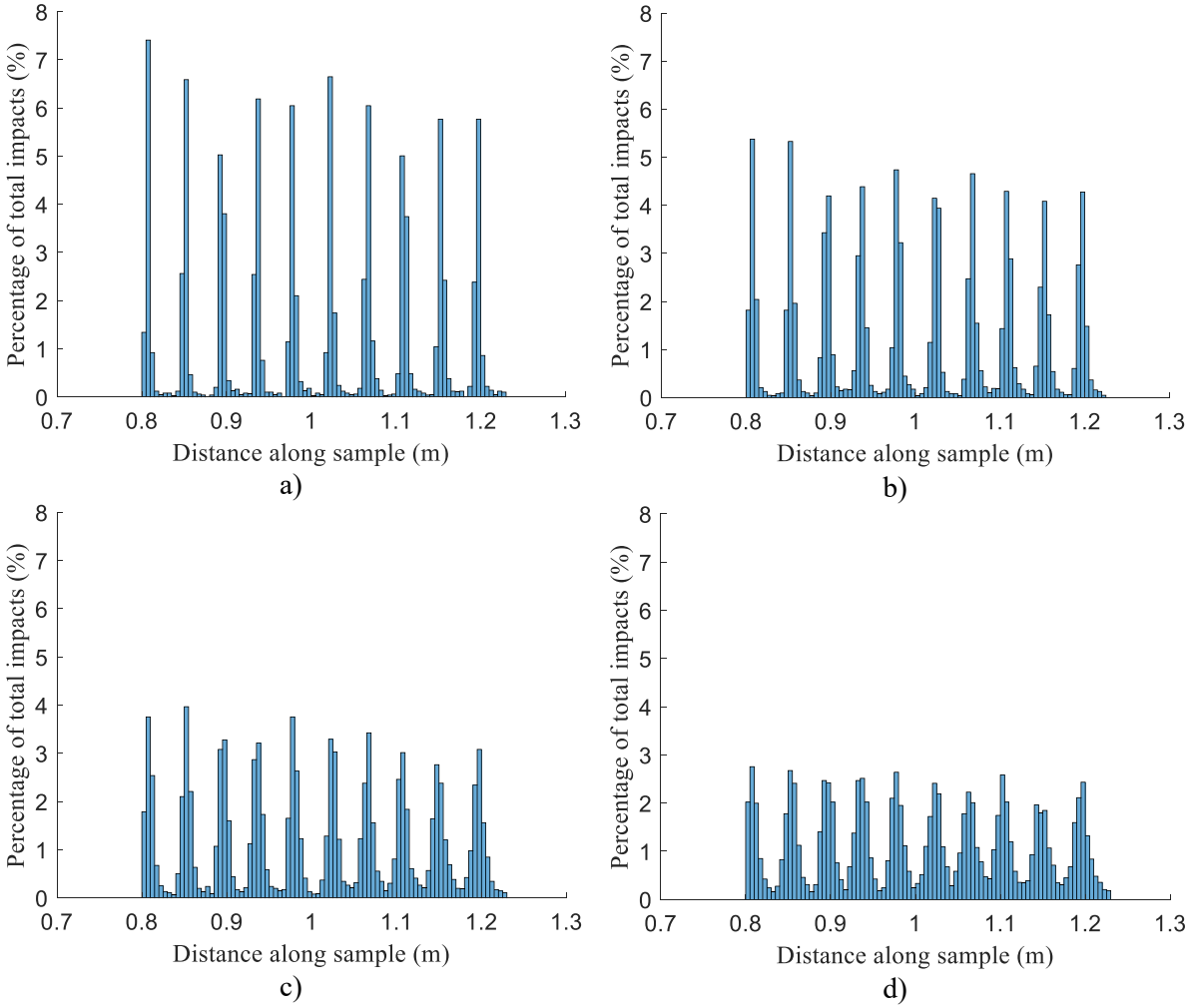

Figure 9. Histograms presenting the droplet impact locations determined computationally at rotational velocities of a) 800 rpm, b) 1000 rpm, c) 1200 rpm and d) 1386 rpm.

3.3. Model Validation

Video recording was not possible in the test rig. Instead, the CFD model was validated by evaluating the kinetic energy of each droplet impact determined computationally against the analytical solution given in DNV-GL-RP-0171. The guideline states that the droplet falling velocity is negligible compared to the sample velocity and therefore the impact velocity, v, of a droplet is given by:

$$v(r) = \omega r, \tag{1}$$

where ω is the rotational velocity of the sample and r is the radial distance of a point from the centre of rotation.

The kinetic energy, E_K, of a droplet can be expressed as:

$$E_K = \frac{1}{12}\rho\pi d^3 v^2, \tag{2}$$

where ρ is the density of the droplet and d is the droplet diameter.

Figure 10 presents the comparison of the kinetic energies of the droplets determined computationally and analytically for a range of rotational velocities. The model gave consistent results with the analytical solution.

4. Rain Erosion Testing Prediction

Rain erosion tests on aluminium samples were conducted with the growth of erosion damage characterised through mass loss and visual inspections. Aluminium exhibits repeatable erosion performance in tests and is defined as the calibration sample in the DNV-GL guidelines. During a whirling arm erosion test on aluminium, the erosion grows linearly from the tip end towards the root. Therefore, the time to damage and the pit depth is directly related to the number of droplets impacting at each point and the kinetic energy of the impact.

Figure 11 presents an aluminium sample after 10 hours at a rotational velocity of 1250 rpm in the ORE Catapult test rig. A droplet diameter of 2.37 mm was used.

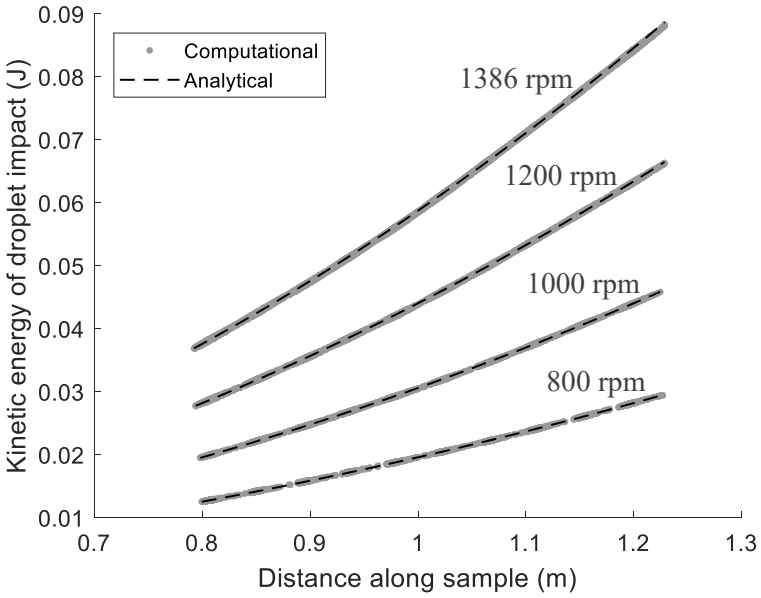

Figure 10. Kinetic energy of droplet impacts determined computationally and analytically at a range of rotational speeds

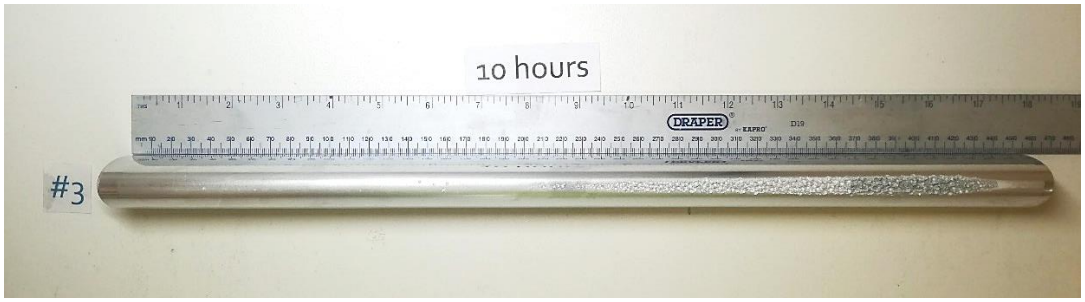

Figure 11. An aluminium sample after 10 hours in the ORE Catapult test rig at a rotational velocity of 1250 rpm.

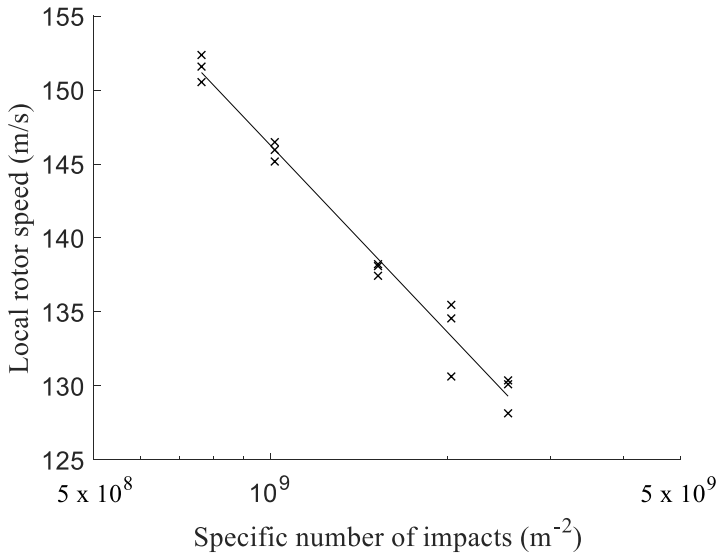

Figure 12. Incubation curve demonstrating the end of incubation at different local velocities on a sample.

Figure 12 presents the incubation curve for the aluminium samples. The recorded ends of the incubation period at different local velocities, and their corresponding kinetic energies, have been expressed in terms of the specific number of droplets impacting the sample.

The incubation curve can be developed into a generalised solution by assuming a power law:

$$N = k{E_k}^m, \tag{3}$$

where N is the specific number of impacts and k and m are constants. This can be transferred into a logarithmic form to calculate the constants k and m.

$$\log N = log\, k + m \log E_k \tag{4}$$

Fitting the test data to equation (4) gives values of -3.77 and 55660 for k and m, respectively.

Combining equation (2) and equation (3) gives:

$$N = k\left(\frac{1}{12}\rho\pi d^3 v^2\right)^m \tag{5}$$

Using equation (5), it now becomes possible to determine the incubation curves for different local velocities and droplet diameters.

The developed equation was then used to predict the damage on identical aluminium samples at a different rotational velocity, but same droplet size and then the same rotational velocity, but a different droplet diameter. A rotational velocity of 1386 rpm and a droplet size of 2.83 mm were used in the two respective rain erosion tests.

Figure 13 presents the predicted incubation curves with the results of the rain erosion tests indicated. The results show that the prediction is effective at identifying the incubation point for the aluminium samples on the ORE Catapult test rig.

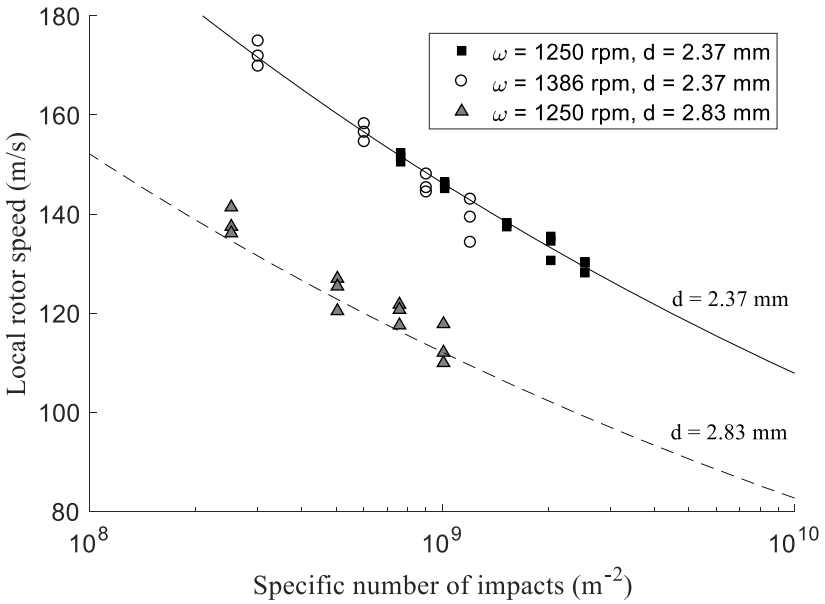

Figure 13. Incubation curves for different rotational velocities and droplet diameters with the test results highlighted.

5. Guideline Comparison

Using the methodology presented in DNV-GL-RP-0171, the two rigs were compared. Tests were performed on coating samples until failure, and on aluminium samples for 6 hours with the mass loss recorded. In both cases, the specific number of impacts was calculated using the DNV-GL guideline.

Figure 14 and Figure 15 present the rain erosion test results of the coating sample after 35 minutes in the ETC rig and 16 hours in the ORE Catapult rig, respectively. Due to the nature of the test rigs, the samples lasted considerably different periods of time. However, under the methodology presented in the DNV-GL guideline the results should be comparable. Table 1 and Table 2 present the results and the comparison between the rigs.

Figure 14. Coating samples after 20 minutes (left) and 35 minutes (right) in the ETC test rig.

Figure 15. Coating sample after 16 hours in the ORE Catapult test rig.

Table 1. Specific number of impacts to failure for the coating samples calculated through DNV-GL-RP-0171.

	ETC Test Rig	ORE Catapult Test Rig
Specific impact frequency [s^{-1} m^{-1}]	30,877	42,699
Time to failure [s]	2,100	57,600
Specific number of impacts [m^{-1}]	64,841,700	2,459,462,400

Table 2. Specific number of impacts after 6 hours for the aluminium samples calculated through DNV-GL-RP-0171 and the corresponding mass loss.

	ETC Test Rig	ORE Catapult Test Rig
Specific impact frequency [s^{-1} m^{-1}]	30,877	57,644
Exposure time [s]	21,600	21,600
Specific number of impacts [m^{-1}]	666,943,200	1,245,110,400
Mass loss [g]	0.05	1.1

The comparison revealed that the coating samples failed after a significantly smaller specific number of impacts in the ETC test rig than in the ORE Catapult test rig. However, the results are reversed for the aluminium samples, with the ETC rig removing less mass than the ORE Catapult rig.

There is also a clear difference in the failure mode of the coating sample in the different test rigs. In the ETC rig the sample exhibits surface pitting, whilst in the ORE Catapult rig the sample experienced subsurface damage that causes large areas of coating to be removed.

The CFD models have revealed that the ORE Catapult test rig has an even aerodynamic flow over the sample, whereas the ETC test rig does not and therefore introduces a high droplet impact density in certain locations. The different characteristics of the two test rigs are thus beneficial for exploring different rain erosion materials and their elastic and viscoelastic properties.

6. Conclusions

The methodology presented enables the prediction of a droplet's impact strike characteristics, the number of impacts and the effect of rig aerodynamics. CFD models for two differing whirling arm test rigs have been developed and validated. The first model was validated against high speed video footage of the corresponding test rig, whilst the second model was validated through a comparison with the predicted kinetic energy of droplet impact against the analytical solution presented in the DNV-GL guideline.

The CFD models revealed that the previous configuration of the ETC test rig introduced aerodynamic droplet concentrations and radial outflow of the droplet path, whilst the ORE Catapult test rig did not. Repeat high speed video characterisation on the modified ETC rig showed droplet break-up still occurred indicating large aerodynamic effects. Rain erosion tests were performed on aluminium samples in the ORE Catapult test rig in line with the DNV-GL guideline. The results of one test were used to successfully predict the result of two subsequent tests performed at different conditions.

Experimental tests on identical coating and aluminium samples were conducted in the ETC rig and the ORE Catapult rig and compared to the DNV-GL guideline. Differing results were seen between the experiments, concluding that the guideline does not provide accurate comparison between test rigs as it does not account for aerodynamic induced droplet effects on the coating damage mode and material response.

The methodology in the guideline has been applied effectively in the ORE Catapult test rig to predict the results of future tests. However, the guideline has been shown to not account for large aerodynamic effects in test rigs and it has been seen that the viscoelastic properties of the rain erosion materials can be influenced by the test droplet impact conditions.

The industry goal is to develop a method for predicting the lifetime of a protection system on a wind turbine from rain erosion test results. This goal is being pursued in the DNV-GL project COBRA.

However, until aerodynamic effects, such as droplet concentration, and viscoelastic material effects are included in tests and lifetime prediction models, the lifetime prediction method is unlikely to be suitable for all test rigs and materials.

Acknowledgements
This work was supported by the Engineering and Physical Sciences Research Council through the EPSRC Centre for Doctoral Training in Composites Manufacture (Grant: EP/K50323X/1), project partners the Offshore Renewable Energy Catapult <https://ore.catapult.org.uk>, and the EPSRC Future Composites Manufacturing Hub (grant: EP/P006701/1). The authors would also like to thank the Wind Blade Research Hub for their support in delivery of this manuscript. All data necessary to reproduce the results and support the conclusions are included within this paper.

References
[1] Keegan M H, Nash D H and Stack M M 2013 On erosion issues associated with the leading edge of wind turbine blades *J. Phys. D. Appl. Phys* **46** 38 p 383001
[2] Zhang S, Dam-Johansen K, Nørkjær S, Bernad P L and Kiil S 2015 Erosion of wind turbine blade coatings - design and analysis of jet-based laboratory equipment for performance evaluation *Prog. Org. Coatings* **78** p 103-115
[3] DNV-GL 2018 Testing of rotor blade erosion protection systems
[4] Frohn A and Roth N 2000 *Dynamics of droplets* Springer-Verlag Berlin Heidelberg